

Accuracy of spike-train Fourier reconstruction for colliding nodes

Andrey Akinshin*, Dmitry Batenkov[†], Yosef Yomdin[‡],

^{*‡}Department of Mathematics,

The Weizmann Institute of Science, Rehovot 76100, Israel

^{*}Laboratory of Inverse Problems of Mathematical Physics,
Sobolev Institute of Mathematics SB RAS, Novosibirsk 630090, Russia

[†]Department of Computer Science,

Technion — Israel Institute of Technology, Haifa 32000, Israel

^{*} Email: andrey.akinshin@weizmann.ac.il

[†] Email: yosef.yomdin@weizmann.ac.il

[‡] Email: batenkov@cs.technion.ac.il

Abstract—We consider signal reconstruction problem for signals F of the form $F(x) = (x) = \sum_{j=1}^d a_j \delta(x - x_j)$, from their Fourier transform $\mathcal{F}(F)(s) = \int_{-\infty}^{\infty} F(x) e^{-isx} dx$. We assume $\mathcal{F}(F)(s)$ to be known for each $s \in [-N, N]$, with an absolute error not exceeding $\epsilon > 0$. We give an absolute lower bound (which is valid with any reconstruction method) for the “worst case” error of reconstruction of F from $\mathcal{F}(F)$, in situations where the nodes x_j are known to form an l elements cluster of a size $h \ll 1$. Using “decimation” algorithm of [6], [7] we provide an upper bound for the reconstruction error, essentially of the same form as the lower one. Roughly, our main result states that for h of order $\frac{1}{N} \epsilon^{\frac{1}{2l-1}}$ the worst case reconstruction error of the cluster nodes is of the same order $\frac{1}{N} \epsilon^{\frac{1}{2l-1}}$, and hence the inside configuration of the cluster nodes (in the worst case scenario) cannot be reconstructed at all. On the other hand, decimation algorithm reconstructs F with the accuracy of order $\frac{1}{N} \epsilon^{\frac{1}{2l}}$.

I. INTRODUCTION

In this paper, we provide lower and upper bounds for the Fourier reconstruction error, in the presence of noise, of spike-train signals in the case of “almost colliding” (or clustering) nodes. The lower bound is obtained via the analysis of the behavior of the Fourier transform under perturbation of the nodes and amplitudes in the cluster, and so it is valid (in the worst case scenario) for any reconstruction method. The upper bound follows from the accuracy analysis of “decimation” reconstruction algorithm, as given in [6], [7].

We hope that our analysis may clarify some aspects of the “Super-resolution problem” for spike-train signals with clustering nodes, as it appears in many old and recent publications on the subject (see, as a very small sample, [12], [13], [17], [19], [20], [23], recent publications [1]–[11], [14]–[16], [18], [21], [22], [26], and references therein).

Let us assume that the signal $F(x)$ is a spike-train, i.e. it is a priori known to be a linear combination of d shifted δ -functions:

$$F(x) = F_{A,X}(x) = \sum_{j=1}^d a_j \delta(x - x_j), \quad (1)$$

where $A = (a_1, \dots, a_d) \in \mathbb{R}^d$, $X = X_d = (x_1, \dots, x_d) \in \mathbb{R}^d$. We shall always assume that $x_1 \leq x_2 \leq \dots \leq x_d$. As for the measurements, we assume that the Fourier transform

$$\mathcal{F}(F)(s) = \int_{-\infty}^{\infty} F(x) e^{-isx} dx \quad (2)$$

is known for each $s \in [-N, N]$, with an absolute error not exceeding $\epsilon > 0$. So our input measurement is a function $\Phi(s)$ satisfying $|\Phi(s) - \mathcal{F}(F)(s)| \leq \epsilon$ for $s \in [-N, N]$.

The first goal of the present paper is to study the “worst case” accuracy of reconstruction of F from $\Phi(s)$ in situations where the nodes x_j are known to form a cluster of a size $h \ll 1$, while being near-uniformly positioned inside the cluster. We give an absolute lower bound for the reconstruction error of the nodes x_j from the measured function $\Phi(s)$, which is valid independently of the reconstruction method applied.

Our second goal is to give an upper bound for the reconstruction error of the nodes x_j , under the same assumptions as above. We show that the decimation algorithm, combined with a homotopy continuation solving of the resulting algebraic equations, as described in [6], [7], produces an error of essentially the same order of magnitude as the lower bound.

Shortly, our main result is as follows:

1. If certain l nodes of F form a cluster of a size $h \sim \frac{1}{N} \epsilon^{\frac{1}{2l-1}}$, while being near-uniformly positioned inside the cluster, then the worst case reconstruction error Δ of the cluster nodes is at least $C h$.
2. If for the same signal F the measurements error is smaller than $\epsilon_1 \sim \epsilon^{\frac{2l}{2l-1}}$ then the decimation algorithm reconstructs the cluster nodes with the error Δ being at most $c h$, $c \ll C$.

The “practical” conclusion could be that the inside configuration of the cluster nodes cannot be reconstructed at all from the Fourier transform $\mathcal{F}(F)(s)$, known with the error ϵ , for $s \in [-N, N]$, if the cluster size h is smaller than $\frac{1}{N} \epsilon^{\frac{1}{2l-1}}$. However, slightly reducing (to ϵ_1) the allowed magnitude of the measurements error, we can accurately and robustly reconstruct the cluster nodes via the decimation algorithm.

The reconstruction error $\Delta \sim \frac{1}{N} \epsilon^{\frac{1}{2l-1}}$ would make practical reconstruction of two colliding nodes very difficult, and of three or more virtually impossible. However, our bound is the worst case one, and one can hope that for a random noise a typical reconstruction accuracy may be much better.

Let us stress that our result is pretty close to the main result of [13], where Fourier sampling of atomic measures on non-uniform grids is studied. In particular, the connection of the form $\epsilon = C(Nh)^{2l-1}$ between the noise, the bandwidth, and the clustering geometry which can be stably recovered, appears also in [13]. Very recently similar bounds were obtained for superresolution of positive sources in [22], and for a Fourier recovery of sparse vectors in [10]. There are also apparent similarities with the classical result of Slepian in [24]. Compare a discussion in [9] of the role of sparsity and clustering, as they appear in the superresolution problem, and, in particular, the discussion in Sections 1.7 and 3.2 of [9] of the “absolute lower bounds” for the reconstruction error. We plan to further investigate the above connections.

II. MAIN RESULT

To state our results we have to make some “normalizing” assumptions on the signal F to be recovered. Indeed, if some amplitudes a_j are small, the reconstruction accuracy of the corresponding nodes drops, while larger a_j imply higher accuracy. So we shall assume that the amplitudes $A = (a_1, \dots, a_d)$ of the signal F satisfy the following assumption $A(m, M)$:

$$0 < m \leq |a_j| \leq M < \infty, \quad j = 1, \dots, d.$$

Definition 2.1: A signal $F_{A,X}$ as given by (1) is said to form an (l, h, ρ) -cluster X if there is an interval $I \subset \mathbb{R}$ of length h which contains exactly l nodes $X_l = \{x_\kappa, x_{\kappa+1}, \dots, x_{\kappa+l-1}\}$ of F , while the minimal distance between the nodes in X_l is at least ρh , $\rho > 0$.

Definition 2.2: For two ordered subsets $V = (v_1, \dots, v_q)$, and $W = (w_1, \dots, w_q)$ in \mathbb{R} the distance $d(V, W)$ is defined as

$$\begin{aligned} d(V, W) &= \max_{s=1}^q |v_s - w_s| = \|v_s - w_s\|_{l^\infty} \geq \\ &\geq \frac{1}{\sqrt{q}} \|v_s - w_s\|_{l^2}. \end{aligned}$$

The following theorem is the first main result of the paper:

Theorem 2.1: Let a signal $F^0 = F_{A^0, X^0}$, satisfying assumption $A(m, M)$, form an (l, h, ρ) -cluster $X_l^0 = \{x_\kappa^0, x_{\kappa+1}^0, \dots, x_{\kappa+l-1}^0\}$. Then there exist parameters A^1, X^1 , satisfying assumption $A(\frac{m}{2}, 2M)$, such that the distance $d(X_l^0, X_l^1)$ between X_l^0 and $X_l^1 = \{x_\kappa^1, x_{\kappa+1}^1, \dots, x_{\kappa+l-1}^1\}$ is at least $C_1 h$, while for $F^1 = F_{A^1, X^1}$, and for each $s \in \mathbb{R}$ with $|s| \leq \frac{1}{2\pi h}$ we have

$$|\mathcal{F}(F^0)(s) - \mathcal{F}(F^1)(s)| \leq C_2 (hs)^{2l-1}. \quad (3)$$

In particular, for $s \in [-N, N]$, $N \leq \frac{1}{2\pi h}$, this difference does not exceed $C_2 (hN)^{2l-1}$. Here the constants C_1 and C_2 depend only on m, M, l, ρ .

The proof of Theorem 2.1 is given in Section III below. From this result we immediately deduce the following:

Corollary 2.1: Assume that the noise $N(s)$ in the Fourier sampling $\mathcal{F}(s)$ on $[-N, N]$ may be an arbitrary function with the only restriction that $|N(s)| \leq \epsilon$, where $0 < \epsilon \ll 1$, and put $h_\epsilon = \frac{1}{N} (\frac{\epsilon}{C_2})^{\frac{1}{2l-1}}$. Let F^0 be any signal, satisfying assumption $A(m, M)$, and forming an (l, h_ϵ, ρ) -cluster X_l^0 . Let F^1 be the new signal produced from F^0 as in Theorem 2.1. Then for any reconstruction algorithm \mathcal{R} the worst-case error in reconstruction of the nodes of either X_l^0 , or of X_l^1 is not smaller than $\frac{1}{2} C_1 h_\epsilon$.

Proof: We pick an “adversary” noise $N(s)$ to be identically zero for the sampling of F^0 and to be equal to $N(s) = \mathcal{F}(F^0)(s) - \mathcal{F}(F^1)(s)$ for the sampling of F^1 . In both cases, by our choice of h_ϵ and by Theorem 2.1, we have $|N(s)| \leq \epsilon$, $s \in [-N, N]$. Notice that for sufficiently small ϵ we have $h_\epsilon \ll \frac{1}{N}$, and hence the condition $N \leq \frac{1}{2\pi h}$ of Theorem 2.1 is satisfied. The measurement results $\Phi(s)$ are identical for F^0 and F^1 , and whatever reconstruction (\hat{A}, \hat{X}) of the signal parameters the algorithm \mathcal{R} produces from $\Phi(s)$, either the distance $d(X_l^0, \hat{X}_l)$, or $d(X_l^1, \hat{X}_l)$, is at least $\frac{1}{2} d(X_l^0, X_l^1)$ which, by Theorem 2.1, is not smaller than $\frac{1}{2} C_1 h_\epsilon$. \square

As for the upper bound on the reconstruction error, we announce the following result:

Theorem 2.2: Let a signal $F^0 = F_{A^0, X^0}$, satisfying assumption $A(m, M)$, form an (l, h, ρ) -cluster $X_l^0 = \{x_\kappa^0, x_{\kappa+1}^0, \dots, x_{\kappa+l-1}^0\}$. Let the measurements error ϵ satisfy $\epsilon \leq \epsilon_1 = C_3 (hN)^{2l}$. Then solving the corresponding decimated Prony system of [6] produces the reconstructed cluster nodes \bar{X}_l^0 with the error at most $\frac{1}{10} \rho h$, i.e. $d(X^0, \bar{X}^0) \leq \frac{1}{10} \rho h$.

In particular, since by the assumptions the distance between the cluster nodes is at least ρh , the number of the nodes, and the inner geometry of the cluster can be robustly restored.

The proof of Theorem 2.2 is based on a combination of the Jacobian estimates in [6], [7] with the “Quantitative Inverse Function theorem” (Theorem 3.2 below). We plan to present the details separately.

III. PROOF OF THEOREM 2.1

We prove Theorem 2.1 in several steps. First, for signals F as above we express the Fourier transform $\mathcal{F}(F)$ through the moments $m_k(F)$.

A. Fourier transform $\mathcal{F}(F)$ and moments $m_k(F)$

For signals F of form (1) their Fourier transform $\mathcal{F}(F)$ can be easily computed explicitly. Let the moments $m_k(F)$ be defined by

$$\begin{aligned} m_k(F_{A,X}) &= \int_{-\infty}^{\infty} x^k F_{A,X}(x) dx = \\ &= \sum_{j=1}^d a_j x_j^k, \quad k = 0, 1, \dots \end{aligned} \quad (1)$$

Proposition 3.1: For $F = F_{A,X} = \sum_{j=1}^d a_j \delta(x - x_j)$ we have

$$\mathcal{F}(F)(s) = \sum_{k=0}^{\infty} \frac{m_k(F)}{k!} \tilde{s}^k, \quad \text{where } \tilde{s} = -2\pi i s. \quad (2)$$

Proof:

$$\begin{aligned}\mathcal{F}(F)(s) &= \int_{-\infty}^{\infty} e^{-2\pi i s x} F(x) dx = \sum_{j=1}^d a_j e^{-2\pi i x_j s} = \\ &= \sum_{j=1}^d a_j \sum_{k=0}^{\infty} \frac{1}{k!} (-2\pi i x_j s)^k = \\ &= \sum_{k=0}^{\infty} \frac{1}{k!} (-2\pi i s)^k \sum_{j=1}^d a_j x_j^k = \\ &= \sum_{k=0}^{\infty} \frac{1}{k!} m_k(F) \tilde{s}^k. \quad \square\end{aligned}$$

Thus the Taylor coefficients of the Fourier transform $\mathcal{F}(F)(s)$ are the consecutive moments $m_k(F)$ divided by $k!$. This fact provides us an ‘‘Algebraic-Geometric’’ approach to the Fourier reconstruction: to produce the signal F^1 starting with F^0 we analyze the behavior of the moments $m_k(F)$, and keep them the same for F^0 and F^1 for $k = 0, 1, \dots, 2l - 2$. This analysis strongly relies on recent results in [4], [5], [7] on the geometry of the ‘‘Prony mapping’’, which is formed by the moments $m_k(F)$.

B. Reduction of Theorem 2.1 to a geometric lemma

The following result is proved in Section III-C below:

Lemma 3.1: Let a signal $F^0 = F_{A^0, X^0}$, satisfying assumption $A(m, M)$, form an $(d, 1, \rho)$ -cluster $X^0 = \{x_1^0, \dots, x_d^0\}$. In other words, all the d nodes of F^0 are ρ -uniformly distributed in the interval $[-\frac{1}{2}, \frac{1}{2}]$. Then there exist parameters A^1, X^1 , satisfying assumption $A(\frac{m}{2}, 2M)$, with $X^1 = (x_1^1, \dots, x_d^1) \subset [-1, 1]$, such that

1. The distance $d(X^0, X^1)$ between the nodes sets X^0 and X^1 is at least $C_1(m, M, d) > 0$.
2. $m_k(F^0) = m_k(F^1)$, $k = 0, 1, \dots, 2d - 2$, where $F_1 = F_{A^1, X^1}$.

Now we can complete the proof of Theorem 2.1. Let a signal $F^0 = F_{A^0, X^0}$, satisfying assumption $A(m, M)$, form an (l, h, ρ) -cluster $X_l^0 = (x_{\kappa}^0, x_{\kappa+1}^0, \dots, x_{\kappa+l-1}^0)$. We rescale the cluster X_l^0 to X_l^0 in the interval $[-\frac{1}{2}, \frac{1}{2}]$, with the same amplitudes A_l^0 . Then we apply Lemma 3.1 (where we put $d = l$), and find the amplitudes A_l^1 and the nodes X_l^1 in the interval $[-1, 1]$, with the same moments as X_l^0 up to $2l - 2$. Applying the inverse scaling, and obtain the cluster $X_l^1 \subset [-h, h]$. Clearly, if the moments were equal before shrinking, they will remain equal afterwards. We extend the cluster X_l^1 with the amplitudes A_l^1 to the required parameters A^1, X^1 , adding the non-cluster nodes of X^0 with their original amplitudes. By Lemma 3.1 the distance $d(X_l^0, X_l^1)$ is at least $C_1 h$, while $m_k(F^0) = m_k(F^1)$, $k = 0, 1, \dots, 2l - 2$.

It remains to show that $|\mathcal{F}(F_{A,X})(s) - \mathcal{F}(F_{\bar{A},\bar{X}})(s)| \leq C_2(hs)^{2l-1}$. By Proposition 3.1 we have

$$\mathcal{F}(F_{A,X})(s) - \mathcal{F}(F_{\bar{A},\bar{X}})(s) = \sum_{k=0}^{\infty} \frac{\gamma_k}{k!} \tilde{s}^k, \quad (3)$$

where $\gamma_k = m_k(F_{A,X}) - m_k(F_{\bar{A},\bar{X}})$, and $\tilde{s} = -2\pi i s$. But by our construction $\gamma_k = 0$, $k = 0, 1, \dots, 2l - 2$. On the other hand, since both X_l and \bar{X}_l are inside $[-h, h]$, while the amplitudes are bounded by $2M$, we have for any k that $|\gamma_k| \leq 4lMh^k := C_3h^k$. So in fact, for $|s| \leq \frac{1}{2\pi h}$ we get

$$\begin{aligned}|\mathcal{F}(F_{A,X})(s) - \mathcal{F}(F_{\bar{A},\bar{X}})(s)| &\leq \sum_{k=2l-1}^{\infty} \frac{C_3}{k!} |\tilde{s}h|^k \leq \\ &\leq C_3(2\pi sh)^{2l-1} \sum_{q=0}^{\infty} \frac{1}{(2l-1+q)!} (2\pi sh)^q \leq \\ &\leq \frac{2C_3(2\pi)^{2l-1}}{(2l-1)!} (sh)^{2l-1} = C_2(sh)^{2l-1},\end{aligned}$$

where we put $C_2 = \frac{2C_3(2\pi)^{2l-1}}{(2l-1)!}$. This completes the proof of Theorem 2.1. \square

C. Proof of Lemma 3.1

Let a signal $F^0 = F_{A^0, X^0}$, satisfying assumption $A(m, M)$, be given, such that all the d nodes of F are ρ -uniformly distributed in the interval $[-\frac{1}{2}, \frac{1}{2}]$. We have to show that there exist parameters A^1, X^1 , satisfying assumption $A(\frac{m}{2}, 2M)$, with $X_d^1 = (x_1^1, \dots, x_d^1) \subset [-1, 1]$, such that the system of equations

$$\begin{aligned}m_k(F^0) &= m_k(F^1), \quad F^1 = F_{A^1, X^1}, \\ k &= 0, 1, \dots, 2d - 2\end{aligned} \quad (4)$$

is satisfied, while the distance $d(X_d^0, X_d^1)$ is at least $C_1(m, M, d) > 0$. In other words, we have to show that the projection of the set $Q \subset \mathbb{R}^d \times \mathbb{R}^d$ consisting of A^1, X^1 which satisfy (4), is large enough.

Let us recall a definition of the Prony mapping $PM : \mathbb{R}^d \times \mathbb{R}^d \rightarrow \mathbb{R}^{2d}$, given in [5]. It is provided by

$$PM(A, X) = (m_0(F_{A,X}), \dots, m_{2d-1}(F_{A,X})) \in \mathbb{R}^{2d}. \quad (5)$$

Put $m_k^0 = m_k(F_{A,X})$. Then $PM(A^0, X^0) = (m_0^0, m_1^0, \dots, m_{2d-1}^0)$. We shall denote by

$$\begin{aligned}\mu &= (\mu_0, \dots, \mu_{2d-1}) = \\ &= (m_0 - m_0^0, m_1 - m_1^0, \dots, m_{2d-1} - m_{2d-1}^0)\end{aligned}$$

the coordinates in \mathbb{R}^{2d} , with the origin shifted to $\mu^0 = PM(A^0, X^0)$. The following result can be easily derived from Theorem 4.5 of [4]:

Theorem 3.1: At each point $(A^0, X^0) \in \mathbb{R}^d \times \mathbb{R}^d$ satisfying conditions of Lemma 3.1, the Jacobian $JPM = JPM(A^0, X^0)$ of the Prony mapping PM is invertible, the norm of its inverse JPM^{-1} is bounded from above by the constant $C_5(m, M, d, \rho)$, and for each $\mu \in \mathbb{C}^{2d}$ we have $\|JPM^{-1}(\mu)\| \geq C_6\|\mu\|$, with a positive $C_6 = C_6(m, M, d, \rho)$.

Let $L = O\mu_{2d-1}$ be the last coordinate axis in \mathbb{R}^{2d} , and let

$$P_X : \mathbb{R}^d \times \mathbb{R}^d \rightarrow \mathbb{R}^d$$

denote the projection of the signal parameters A, X to the nodes coordinates X . Then for each $\mu \in L$ we have $\|P \circ JPM^{-1}(\mu)\| \geq C_7\|\mu\|$, with a positive $C_7 = C_7(m, M, d, \rho)$.

Proof: The first three statements of Theorem 3.1 follow directly from Theorem 4.5 of [4]. The last statement follows from the fact that for the fixed nodes the restriction of the first d coordinates of the Prony mapping PM , and hence, of its Jacobian JPM , to the coefficients A is a non-degenerate linear mapping to \mathbb{R}^d , with the Vandermonde matrix on the nodes X . Hence, the pre-image $JPM^{-1}(L)$ cannot be contained in $\mathbb{R}^d \times \{0\} \subset \mathbb{R}^d \times \mathbb{R}^d$. Otherwise at least one of the first d moments would change along L . In fact, it is easy to show that the line $JPM^{-1}(L)$ forms a positive angle with $\mathbb{R}^d \times \{0\}$, which is bounded from below by a constant depending only on m, M, d, ρ . But this is equivalent to the last statement of Theorem 3.1. \square

On the other hand, using the standard solution procedure of the Prony system, one can easily show the following fact:

Proposition 3.2: There are constants $R_1 = R_1(m, M, d, \rho)$ and $C_8 = C_8(m, M, d, \rho)$, such that for each point $(A^0, X^0) \in \mathbb{R}^d \times \mathbb{R}^d$, satisfying conditions of Lemma 3.1, the first and the second derivatives of the Prony mapping PM are bounded by C_8 in the ball B_{R_1} in $\mathbb{R}^d \times \mathbb{R}^d$ centered at (A^0, X^0) .

With these two preparatory results we now apply the following “Quantitative Inverse Function Theorem” (see. e.g. [25]):

Theorem 3.2: Let $G : (B_1^m, 0) \rightarrow (\mathbb{R}^m, 0)$ be a twice differentiable mapping of the unit ball B_1^m at the origin in \mathbb{R}^m to \mathbb{R}^m , with $G(0) = 0$, such that the Jacobian $J = JG(0)$ is invertible, and $\|J^{-1}\| \leq K_1 < \infty$. Assume that the second derivatives of G are bounded by K_2 in the ball B_1^m . Then the inverse mapping G^{-1} exists in the ball $B_{R_2}^m$ of radius R_2 , centered at $0 \in \mathbb{R}^m$, and satisfies there the condition

$$\|G^{-1}(x) - J^{-1}(x)\| \leq C_9(m, K_1, K_2)\|x\|^2, \quad (6)$$

for $x \in B_{R_2}^m$,

with $R_2 = R_2(m, K_1, K_2)$ and $C_9 = C_9(m, K_1, K_2)$ depending only on m, K_1 , and K_2 .

We apply Theorem 3.2, properly rescaled, to the the Prony mapping PM in the ball B_{R_1} in $\mathbb{R}^d \times \mathbb{R}^d$ centered at (A^0, X^0) , with the bounds provided by Theorem 3.1 and Proposition 3.2. We conclude that in the ball B_{R_3} of radius R_3 at the point $\mu^0 = PM(A^0, X^0) \in \mathbb{R}^{2d}$ the inverse PM^{-1} exists and satisfies

$$\|PM^{-1}(\mu) - J^{-1}(\mu)\| \leq C_{10}\|\mu\|^2, \quad (7)$$

where $J = JPM$ is the Jacobian of the Prony mapping PM at (A^0, X^0) , and the constants R_3 and C_{10} depend only on m, M, d, ρ .

From the last statement of Theorem 3.1 we get for $\mu \in L = O\mu_{2d-1}$

$$\|P \circ J^{-1}(\mu)\| \geq C_{11}\|\mu\|, \quad (8)$$

with P the projection of the signal parameters A, X to the nodes X , and $C_{11} = C_{11}(m, M, d, \rho)$ a positive constant.

Finally we put $\mu^1 = (0, \dots, 0, \eta)$, with $\eta = \min(R_3, \frac{C_{11}}{2C_{10}})$, and take (A^1, X^1) to be the inverse image $PM^{-1}(\mu^1)$. By the construction we have

$$m_k(F^0) = m_k(F^1), \quad k = 0, 1, \dots, 2d - 2. \quad (9)$$

On the other hand, $X^1 = P(PM^{-1}(\mu^1)) = P(J^{-1}(\mu^1) - w)$, where $w = J^{-1}(\mu^1) - PM^{-1}(\mu^1)$, and hence, by (7), we have $\|w\| \leq C_{10}\|\mu^1\|^2 = C_{10}\eta^2$. By (8) we get $\|P \circ J^{-1}(\mu^1)\| \geq C_{11}\eta$, and therefore

$$\begin{aligned} \|X^1\| &= \|P(J^{-1}(\mu^1) - w)\| \geq C_{11}\eta - C_{10}\eta^2 = \\ &= \eta(C_{11} - C_{10}\eta) \geq \eta \frac{C_{11}}{2} := C_{12}. \end{aligned}$$

The norm $\|X^1\|$ of X^1 here is the l^2 norm with respect to the coordinates in \mathbb{R}^d centered at X^0 . Hence $\frac{1}{\sqrt{d}}\|X^1\|$ bounds from below the distance $d(X^0, X^1)$. This completes the proof of Lemma 3.1, with $C_1 = \frac{1}{\sqrt{d}}C_{12}$. \square

Remark. In this paper we consider only the curve $PM^{-1}(L)$ where the first $2l - 2$ moments m_k take equal value. In the direction of this curve the magnification of the measurements error is maximal. In fact, for each $q = 1, \dots, 2l - 2$ there is a stratum Σ_q in $\mathbb{R}^d \times \mathbb{R}^d$, of dimension $2l - q - 1$, where the first q moments m_k take equal value. In the direction of this stratum the error magnification is of order $q + 1$. The geometry of the strata Σ_q plays important role in the understanding of the error magnification patterns which occur in the Fourier reconstruction of spike-trains. We plan to present the results in this direction separately.

SOME EXAMPLES

The following examples illustrate the shape and behavior of the signals F_q^0 and F_q^1 , $q = 1, 3, 5$, for which the difference $DF_q(s) = \mathcal{F}(F_q^0)(s) - \mathcal{F}(F_q^1)(s)$ between their Fourier transforms is of order q in s . As it was explained above, the geometry of the strata Σ_q , containing F_q plays important role in the error magnification which occurs in the Fourier reconstruction of spike-trains.

We consider signals with $d = 3$ nodes of the form (1): $F_q(x) = \sum_{j=1}^3 a_{qj}\delta(x - x_{qj})$. Their specific parameters are shown in table I. In this table we assume h to be fixed, and put $\eta = \tilde{\eta}h$, with $\tilde{\eta}$ being the “free parameter along the stratum Σ_q ”. The maximal distance between the nodes of F_q^0 and F_q^1 in each case is 2η .

Table II shows the difference between the moments m_0, m_1, m_2, m_3, m_4 of F_q^0 and F_q^1 . We see that this difference is zero exactly for the first q moments, $q = 1, 3, 5$. Figure 1 shows the difference $DF_q(s) = \mathcal{F}(F_q^0)(s) - \mathcal{F}(F_q^1)(s)$, for the frequency $s \in [0, 1]$. The normalized difference presented on the ordinate is $\frac{DF}{h}$. In this figure we fix $\eta = 0.05, h = 0.1$.

ACKNOWLEDGMENT

This research was supported by the ISF Grant No. 779/13.

TABLE I
SIGNALS PARAMETERS

	a_1	a_2	a_3	x_1	x_2	x_3
F_1^0	1	1	1	$-h - \eta$	$-\eta$	$+h + \eta$
F_1^1	1	1	1	$-h - \eta$	$+\eta$	$+h + \eta$
F_3^0	1	1	1	$-h - \eta$	$-\eta$	$+h + 2\eta$
F_3^1	1	1	1	$-h - 2\eta$	$+\eta$	$+h + \eta$
F_5^0	$-1 - 3\bar{\eta}$	$2 + 3\bar{\eta}$	-1	$-h - \eta$	$-\eta$	$h + 2\eta$
F_5^1	-1	$2 + 3\bar{\eta}$	$-1 - 3\bar{\eta}$	$-h - 2\eta$	$+\eta$	$+h + \eta$

TABLE II
MOMENTS DIFFERENCES

	Δm_0	Δm_1	Δm_2	Δm_3	Δm_4
F_1	0	2η	0	$2\eta^3$	0
F_3	0	0	0	$6h^2\eta + 18h\eta^2 + 16\eta^3$	0
F_5	0	0	0	0	0

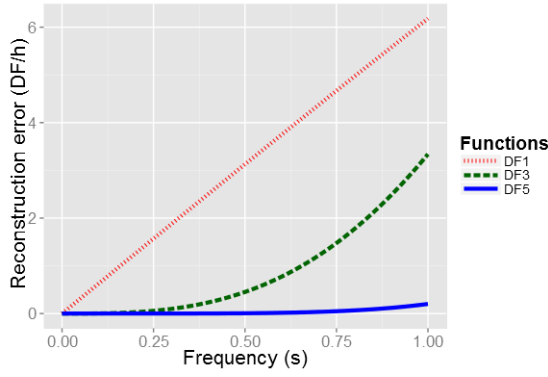


Fig. 1. Fourier differences DF of the signals from Table I.

REFERENCES

- [1] J.-M. Azaïs, Y. de Castro, and F. Gamboa, "Spike detection from inaccurate samplings," *Applied and Computational Harmonic Analysis*, in press. [Online]. Available: <http://www.sciencedirect.com/science/article/pii/S106352031400044X>
- [2] D. Batenkov, N. Sarig, and Y. Yomdin, "Accuracy of algebraic Fourier reconstruction for shifts of several signals," *Sampling Theory in Signal and Image Processing*, vol. 13, no. 2, pp. 151–173, 2014.
- [3] D. Batenkov and Y. Yomdin, "Algebraic signal sampling, Gibbs phenomenon and Prony-type systems," in *Proceedings of the 10th International Conference on Sampling Theory and Applications (SAMPTA)*, 2013.
- [4] —, "On the accuracy of solving confluent Prony systems," *SIAM J. Appl. Math.*, vol. 73, no. 1, pp. 134–154, 2013.
- [5] —, "Geometry and Singularities of the Prony mapping," *Journal of Singularities*, vol. 10, pp. 1–25, 2014.
- [6] D. Batenkov, "Accurate solution of near-colliding Prony systems via decimation and homotopy continuation," *arXiv:1501.00160 [cs, math]*, Dec. 2014, arXiv: 1501.00160. [Online]. Available: <http://arxiv.org/abs/1501.00160>
- [7] —, "Numerical stability bounds for algebraic systems of Prony type and their accurate solution by decimation," *arXiv preprint arXiv:1409.3137*, 2014. [Online]. Available: <http://arxiv.org/abs/1409.3137>
- [8] E. J. Candès and C. Fernandez-Granda, "Super-Resolution from Noisy Data," *Journal of Fourier Analysis and Applications*, vol. 19,

- no. 6, pp. 1229–1254, Dec. 2013. [Online]. Available: <http://link.springer.com/article/10.1007/s00041-013-9292-3>
- [9] —, "Towards a Mathematical Theory of Super-resolution," *Communications on Pure and Applied Mathematics*, vol. 67, no. 6, pp. 906–956, Jun. 2014. [Online]. Available: <http://onlinelibrary.wiley.com/doi/10.1002/cpa.21455/abstract>
- [10] L. Demanet and N. Nguyen, "The recoverability limit for superresolution via sparsity," *Preprint*, 2014.
- [11] L. Demanet, D. Needell, and N. Nguyen, "Super-resolution via superset selection and pruning," in *Proceedings of the 10th International Conference on Sampling Theory and Applications (SAMPTA)*, 2013.
- [12] D. L. Donoho and P. B. Stark, "Uncertainty principles and signal recovery," *SIAM J. Appl. Math.*, vol. 49, pp. 906–931, 1989.
- [13] D. Donoho, "Superresolution via sparsity constraints," *SIAM Journal on Mathematical Analysis*, vol. 23, no. 5, pp. 1309–1331, 1992.
- [14] V. Duval and G. Peyré, "Exact support recovery for sparse spikes deconvolution," *arXiv preprint arXiv:1306.6909*, 2013. [Online]. Available: <http://arxiv.org/abs/1306.6909>
- [15] C. Fernandez-Granda, "Support detection in super-resolution," in *Proc. of 10th Sampling Theory and Applications (SAMPTA)*, 2013, pp. 145–148. [Online]. Available: <http://arxiv.org/abs/1302.3921>
- [16] R. Heckel, V. I. Morgenshtern, and M. Soltanolkotabi, "Super-Resolution Radar," *arXiv:1411.6272 [cs, math]*, Nov. 2014, arXiv: 1411.6272. [Online]. Available: <http://arxiv.org/abs/1411.6272>
- [17] S. Levy and P. K. Fullagar, "Reconstruction of a sparse spike train from a portion of its spectrum and application to high-resolution deconvolution," *Geophysics*, vol. 46, no. 9, pp. 1235–1243, 1981.
- [18] W. Liao and A. Fannjiang, "MUSIC for Single-Snapshot Spectral Estimation: Stability and Super-resolution," *arXiv:1404.1484 [cs, math]*, Apr. 2014. [Online]. Available: <http://arxiv.org/abs/1404.1484>
- [19] C. W. McCutchen, "Superresolution in microscopy and the Abbe resolution limit," *J. Opt. Soc. Am.*, vol. 57, no. 10, pp. 1190–1190, 1967.
- [20] K. Minami, S. Kawata, and S. Minami, "Superresolution of Fourier Transform spectra by autoregressive model fitting with singular value decomposition," *Appl. Optics*, vol. 24, pp. 162–167, 1985.
- [21] A. Moitra, "The Threshold for Super-resolution via Extremal Functions," *arXiv:1408.1681 [cs, math, stat]*, Aug. 2014, arXiv: 1408.1681. [Online]. Available: <http://arxiv.org/abs/1408.1681>
- [22] V. I. Morgenshtern and E. J. Candès, "Stable super-resolution of positive sources: the discrete setup," *Preprint*, 2014.
- [23] J. Odendaal, E. Barnard, and C. W. I. Pistorius, "Two-dimensional superresolution radar imaging using the MUSIC algorithm," *IEEE Transactions on Antennas and Propagation*, vol. 42, no. 10, pp. 1386–1391, 1994.
- [24] D. Slepian, "Prolate spheroidal wave functions," *Fourier Analysis and uncertainty, V - The discrete case. Bell System Technical Journal*, vol. 57, pp. 1371–1430, 1978.
- [25] Y. Yomdin, "Some quantitative results in singularity theory," *Ann. Polon. Math.*, vol. 87, pp. 277–299, 2005.
- [26] —, "Singularities in algebraic data acquisition," *Real and complex singularities, London Math. Soc. Lecture Note Ser.*, vol. 380, pp. 378–396, 2010.